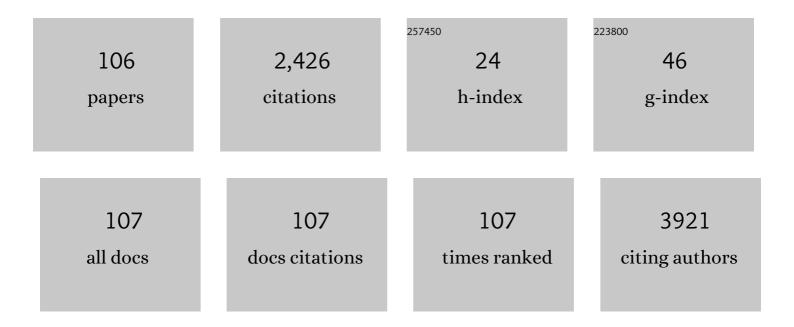
Inhee Choi

List of Publications by Year in descending order

Source: https://exaly.com/author-pdf/3351460/publications.pdf Version: 2024-02-01



#	Article	IF	CITATIONS
1	Sensitive and Homogeneous Surfaceâ€Enhanced Raman Scattering Detection Using Heterometallic Interfaces on Metal–Organic Frameworkâ€Derived Structure. Advanced Materials Interfaces, 2022, 9, .	3.7	6
2	Gold and silver plasmonic nanoprobes trace the positions of histone codes. BMB Reports, 2022, 55, 111-112.	2.4	0
3	Optical Detection of Copper Ions <i>via</i> Structural Dissociation of Plasmonic Sugar Nanoprobes. Analytical Chemistry, 2022, 94, 5521-5529.	6.5	14
4	Redox/pH-dual responsive functional hollow silica nanoparticles for hyaluronic acid-guided drug delivery. Journal of Industrial and Engineering Chemistry, 2022, 108, 72-80.	5.8	19
5	Colloidal Multiscale Assembly via Photothermally Driven Convective Flow for Sensitive Inâ€Solution Plasmonic Detections. Small, 2022, 18, e2201075.	10.0	5
6	Ultrasensitive and real-time optical detection of cellular oxidative stress using graphene-covered tunable plasmonic interfaces. Nano Convergence, 2022, 9, .	12.1	2
7	Extra- and Intracellular Monitoring of TGF-β Using Single Immunoplasmonic Nanoprobes. ACS Sensors, 2021, 6, 1823-1830.	7.8	6
8	Sensitive and Direct Optical Monitoring of Release and Cellular Uptake of Aqueous CO from CO-Releasing Molecules. Analytical Chemistry, 2021, 93, 9927-9932.	6.5	3
9	High-spatial and colourimetric imaging of histone modifications in single senescent cells using plasmonic nanoprobes. Nature Communications, 2021, 12, 5899.	12.8	3
10	Induction of crystal nucleation by orientation-controlled binding of His ₆ -tagged proteins to functionalized gold nanoparticles. CrystEngComm, 2020, 22, 1032-1040.	2.6	0
11	Aqueous-Phase Synthesis of Hyaluronic Acid-Based Hydrogel Nanoparticles for Molecular Storage and Enzymatic Release. ACS Applied Polymer Materials, 2020, 2, 342-350.	4.4	5
12	Graphene oxide-induced neurotoxicity on neurotransmitters, AFD neurons and locomotive behavior in Caenorhabditis elegans. NeuroToxicology, 2020, 77, 30-39.	3.0	23
13	Identification of adverse outcome pathway related to high-density polyethylene microplastics exposure: Caenorhabditis elegans transcription factor RNAi screening and zebrafish study. Journal of Hazardous Materials, 2020, 388, 121725.	12.4	34
14	Dual Mode Rapid Plasmonic Detections of Chemical Disinfectants (CMIT/MIT) Using Target-Mediated Selective Aggregation of Gold Nanoparticles. Analytical Chemistry, 2020, 92, 4201-4208.	6.5	17
15	Intracellular Nanomaterial Delivery <i>via</i> Spiral Hydroporation. ACS Nano, 2020, 14, 3048-3058.	14.6	45
16	Adjustable and Versatile 3D Tumor Spheroid Culture Platform with Interfacial Elastomeric Wells. ACS Applied Materials & Interfaces, 2020, 12, 6924-6932.	8.0	20
17	Active Surface Hydrophobicity Switching and Dynamic Interfacial Trapping of Microbial Cells by Metal Nanoparticles for Preconcentration and In-Plane Optical Detection. Nano Letters, 2019, 19, 7449-7456.	9.1	9
18	Optical Detection of Small Metabolites for Biological Gas Conversion by using Metal Nanoparticle Monolayers Produced by Capillary-Assisted Transfer. Analytical Chemistry, 2019, 91, 13152-13157.	6.5	0

#	Article	IF	CITATIONS
19	Photothermally Enhanced Molecular Delivery and Cellular Positioning on Patterned Plasmonic Interfaces. ACS Applied Materials & Interfaces, 2019, 11, 36420-36427.	8.0	8
20	Phase transfer-driven rapid and complete ligand exchange for molecular assembly of phospholipid bilayers on aqueous gold nanocrystals. Chemical Communications, 2019, 55, 3195-3198.	4.1	9
21	Fabrication Strategies of 3D Plasmonic Structures for SERS. Biochip Journal, 2019, 13, 30-42.	4.9	36
22	Multifunctional and recyclable TiO2 hybrid sponges for efficient sorption, detection, and photocatalytic decomposition of organic pollutants. Journal of Industrial and Engineering Chemistry, 2019, 73, 328-335.	5.8	20
23	On-chip plasmonic immunoassay based on targeted assembly of gold nanoplasmonic particles. Analyst, The, 2019, 144, 2820-2826.	3.5	7
24	Facile Amplification of Solution-State Surface-Enhanced Raman Scattering of Small Molecules Using Spontaneously Formed 3D Nanoplasmonic Wells. Analytical Chemistry, 2018, 90, 5023-5031.	6.5	21
25	Tunable Plasmonic Cavity for Label-free Detection of Small Molecules. ACS Applied Materials & Interfaces, 2018, 10, 13226-13235.	8.0	33
26	Developing adverse outcome pathways on silver nanoparticle-induced reproductive toxicity via oxidative stress in the nematode <i>Caenorhabditis elegans</i> using a Bayesian network model. Nanotoxicology, 2018, 12, 1182-1197.	3.0	29
27	Photothermal Convection Lithography for Rapid and Direct Assembly of Colloidal Plasmonic Nanoparticles on Generic Substrates. Small, 2018, 14, e1803055.	10.0	37
28	Controlled drug release with surface-capped mesoporous silica nanoparticles and its label-free in situ Raman monitoring. European Journal of Pharmaceutics and Biopharmaceutics, 2018, 131, 232-239.	4.3	15
29	Facile Fabrication of Large-Scale Porous and Flexible Three-Dimensional Plasmonic Networks. ACS Applied Materials & Interfaces, 2018, 10, 28242-28249.	8.0	12
30	3D Assembly of Metal Nanoparticles at Oleic Acid/Water Interface via Their Autonomous and Rapid Interfacial Locomotion. Advanced Materials Interfaces, 2018, 5, 1800981.	3.7	4
31	DPP-IV Inhibitory Potentials of Flavonol Glycosides Isolated from the Seeds of Lens culinaris: In Vitro and Molecular Docking Analyses. Molecules, 2018, 23, 1998.	3.8	57
32	High-throughput drug screening using the Ebola virus transcription- and replication-competent virus-like particle system. Antiviral Research, 2018, 158, 226-237.	4.1	19
33	Gold Nanoparticles as Nucleation-Inducing Reagents for Protein Crystallization. Crystal Growth and Design, 2017, 17, 497-503.	3.0	14
34	Rapid and high-throughput colorimetric screening for anti-aggregation reagents of protein conformational diseases by using gold nanoplasmonic particles. Nanomedicine: Nanotechnology, Biology, and Medicine, 2017, 13, 1575-1585.	3.3	4
35	Determination of nanomolar levels of reactive oxygen species in microorganisms and aquatic environments using a single nanoparticle-based optical sensor. Analytica Chimica Acta, 2017, 967, 85-92.	5.4	8
36	A gold nanoparticle-mediated rapid in vitro assay of anti-aggregation reagents for amyloid β and its validation. Chemical Communications, 2017, 53, 4449-4452.	4.1	12

#	Article	IF	CITATIONS
37	Real-Time Optical Monitoring of Pt Catalyst Under the Potentiodynamic Conditions. Scientific Reports, 2016, 6, 38847.	3.3	0
38	Integrated Microalgae Analysis Photobioreactor for Rapid Strain Selection. ACS Nano, 2016, 10, 5635-5642.	14.6	3
39	Recent Advances in Nanoplasmonic Sensors for Environmental Detection and Monitoring. Journal of Nanoscience and Nanotechnology, 2016, 16, 4274-4283.	0.9	14
40	Spontaneous Self-Formation of 3D Plasmonic Optical Structures. ACS Nano, 2016, 10, 7639-7645.	14.6	25
41	Ultrafast colorimetric determination of predominant protein structure evolution with gold nanoplasmonic particles. Nanoscale, 2016, 8, 1952-1959.	5.6	10
42	A single nanoparticle-based sensor for hydrogen peroxide (H ₂ O ₂) via cytochrome c-mediated plasmon resonance energy transfer. Chemical Communications, 2015, 51, 15370-15373.	4.1	26
43	Solution based, on chip direct growth of three-dimensionally wrinkled gold nanoparticles for a SERS active substrate. Chemical Communications, 2015, 51, 213-216.	4.1	14
44	Graphene Nanopore with Self-Aligned Plasmonic Optical Antenna. Biophysical Journal, 2014, 106, 414a.	0.5	2
45	Graphene Nanopore with a Self-Integrated Optical Antenna. Nano Letters, 2014, 14, 5584-5589.	9.1	79
46	On-Chip Fast Plasmonic Detection of Single Molecule Mirna for Cancer Diagnosis. Biophysical Journal, 2014, 106, 617a.	0.5	1
47	Rapid Detection of Protein Aggregation and Inhibition by Dual Functions of Gold Nanoplasmonic Particles: Catalytic Activator and Optical Reporter. Biophysical Journal, 2014, 106, 416a-417a.	0.5	4
48	Interfacial liquid-state surface-enhanced Raman spectroscopy. Nature Communications, 2013, 4, 2182.	12.8	117
49	On-Chip Colorimetric Detection of Cu ²⁺ lons via Density-Controlled Plasmonic Core–Satellites Nanoassembly. Analytical Chemistry, 2013, 85, 7980-7986.	6.5	31
50	Current nano/biotechnological approaches in amyotrophic lateral sclerosis. Biomedical Engineering Letters, 2013, 3, 209-222.	4.1	5
51	Label-free electrochemical monitoring of vasopressin in aptamer-based microfluidic biosensors. Analytica Chimica Acta, 2013, 759, 74-80.	5.4	38
52	Rapid Detection of AÎ ² Aggregation and Inhibition by Dual Functions of Gold Nanoplasmic Particles: Catalytic Activator and Optical Reporter. ACS Nano, 2013, 7, 6268-6277.	14.6	56
53	Real-time analysis and direct observations of different superoxide dismutase (SOD1) molecules bindings to aggregates in temporal evolution step. Colloids and Surfaces B: Biointerfaces, 2013, 101, 266-271.	5.0	10
54	Plasmonic Nanosensors: Review and Prospect. IEEE Journal of Selected Topics in Quantum Electronics, 2012, 18, 1110-1121.	2.9	94

#	Article	IF	CITATIONS
55	Colorimetric tracking of protein structural evolution based on the distance-dependent light scattering of embedded gold nanoparticles. Chemical Communications, 2012, 48, 2286.	4.1	15
56	Three-Dimensional Reduced-Symmetry of Colloidal Plasmonic Nanoparticles. Nano Letters, 2012, 12, 2436-2440.	9.1	29
57	Core–Satellites Assembly of Silver Nanoparticles on a Single Gold Nanoparticle via Metal Ion-Mediated Complex. Journal of the American Chemical Society, 2012, 134, 12083-12090.	13.7	68
58	Ultra-sensitive, label-free probing of the conformational characteristics of amyloid beta aggregates with a SERS active nanofluidic device. Microfluidics and Nanofluidics, 2012, 12, 663-669.	2.2	51
59	Size-selective concentration and label-free characterization of protein aggregates using a Raman active nanofluidic device. Lab on A Chip, 2011, 11, 632-638.	6.0	49
60	Lipid molecules induce the cytotoxic aggregation of Cu/Zn superoxide dismutase with structurally disordered regions. Biochimica Et Biophysica Acta - Molecular Basis of Disease, 2011, 1812, 41-48.	3.8	23
61	Formation of abnormally large-sized tubular amyloid β aggregates on a nanostructured gold surface. Korean Journal of Chemical Engineering, 2011, 28, 184-188.	2.7	0
62	Innentitelbild: Simultaneous Optical Monitoring of the Overgrowth Modes of Individual Asymmetric Hybrid Nanoparticles (Angew. Chem. 20/2011). Angewandte Chemie, 2011, 123, 4614-4614.	2.0	2
63	Simultaneous Optical Monitoring of the Overgrowth Modes of Individual Asymmetric Hybrid Nanoparticles. Angewandte Chemie - International Edition, 2011, 50, 4633-4636.	13.8	12
64	Inside Cover: Simultaneous Optical Monitoring of the Overgrowth Modes of Individual Asymmetric Hybrid Nanoparticles (Angew. Chem. Int. Ed. 20/2011). Angewandte Chemie - International Edition, 2011, 50, 4520-4520.	13.8	0
65	Direct Observation of Defects and Increased Ion Permeability of a Membrane Induced by Structurally Disordered Cu/Zn-Superoxide Dismutase Aggregates. PLoS ONE, 2011, 6, e28982.	2.5	15
66	Colorimetric Determination of pH Values using Silver Nanoparticles Conjugated with Cytochrome c. Bulletin of the Korean Chemical Society, 2011, 32, 3433-3436.	1.9	5
67	10.2478/s11814-009-0314-4. , 2011, 27, 324.		0
68	Selective Aggregation of Polyanion-Coated Gold Nanorods Induced by Divalent Metal Ions in an Aqueous Solution. Journal of Nanoscience and Nanotechnology, 2010, 10, 3538-3542.	0.9	6
69	Dependence of approaching velocity on the force-distance curve in AFM analysis. Korean Journal of Chemical Engineering, 2010, 27, 324-327.	2.7	6
70	Picomolar selective detection of mercuric ion (Hg ^{2 +}) using a functionalized single plasmonic gold nanoparticle. Nanotechnology, 2010, 21, 145501.	2.6	25
71	Development of a novel biosensor for in-vitro observation of protein behaviors. , 2009, , .		0
72	Biomimetic sensors for the heavy metal detection. , 2009, , .		1

Biomimetic sensors for the heavy metal detection. , 2009, , . 72

#	Article	IF	CITATIONS
73	Effect of laser beam focusing point on AFM measurements. Korean Journal of Chemical Engineering, 2009, 26, 496-499.	2.7	2
74	Fabrication of multicomponent protein microarrays with microfluidic devices of poly(dimethylsiloxane). Macromolecular Research, 2009, 17, 192-196.	2.4	11
75	Highly selective detection of Cu2+ utilizing specific binding between Cu-demetallated superoxide dismutase 1 and the Cu2+ ion via surface plasmon resonance spectroscopy. Chemical Communications, 2009, , 6171.	4.1	20
76	Sensitive and Colorimetric Detection of the Structural Evolution of Superoxide Dismutase with Gold Nanoparticles. Analytical Chemistry, 2009, 81, 1378-1382.	6.5	76
77	Highly selective modification of silicon oxide structures fabricated by an AFM anodic oxidation. Korean Journal of Chemical Engineering, 2008, 25, 386-389.	2.7	2
78	Fabrication of island-type microelectrode via AFM lithography for a highly sensitive Pt-ion detection system. Sensors and Actuators B: Chemical, 2008, 129, 734-740.	7.8	4
79	Label-free sensitive optical detection of polychlorinated biphenyl (PCB) in an aqueous solution based on surface plasmon resonance measurements. Sensors and Actuators B: Chemical, 2008, 134, 300-306.	7.8	20
80	Investigation on shape variation of Au nanocrystals. Current Applied Physics, 2008, 8, 810-813.	2.4	5
81	Fabrication of hierarchical micro/nanostructures via scanning probe lithography and wet chemical etching. Ultramicroscopy, 2008, 108, 1205-1209.	1.9	17
82	Construction of pcAFM module to measure photoconductance with a nanoscale spatial resolution. Ultramicroscopy, 2008, 108, 1090-1093.	1.9	6
83	Directed Positioning of Single Cells in Microwells Fabricated by Scanning Probe Lithography and Wet Etching Methods. Langmuir, 2008, 24, 2597-2602.	3.5	16
84	Fast image scanning method in liquid-AFM without image distortion. Nanotechnology, 2008, 19, 445701.	2.6	8
85	Urea-Driven Conformational Changes in Surface-Bound Superoxide Dismutase. Bulletin of the Korean Chemical Society, 2008, 29, 1451-1458.	1.9	4
86	Observation on Growth Process of Gold Y- and haped Nanoparticles in Solutions. Journal of Nanoscience and Nanotechnology, 2007, 7, 3823-3826.	0.9	0
87	Fabrication of 3D Functionalized Microstructure via Scanning Probe Lithography and Self-Assembly Methods. Journal of Nanoscience and Nanotechnology, 2007, 7, 4161-4164.	0.9	2
88	Interfacial kinetic enhancement of metal ion adsorption on binary mixed self-assembled monolayers. Applied Surface Science, 2007, 253, 7554-7558.	6.1	6
89	In situ observation of the behavior of superoxide dismutase aggregates on a patterned surface via scanning probe microscopy. Microelectronic Engineering, 2007, 84, 1766-1769.	2.4	0
90	Fabrication of a 3-dimensional microstructure by sequential anodic oxidation (SAO). Microelectronic Engineering, 2007, 84, 308-312.	2.4	2

INHEE CHOI

#	Article	IF	CITATIONS
91	Fabrication of 3D functionalized microstructure via scanning probe lithography and self-assembly methods. Journal of Nanoscience and Nanotechnology, 2007, 7, 4161-4.	0.9	0
92	Reversible pH-Driven Conformational Switching of Tethered Superoxide Dismutase with Gold Nanoparticle Enhanced Surface Plasmon Resonance Spectroscopy. Journal of the American Chemical Society, 2006, 128, 12870-12878.	13.7	66
93	Phase Separation of a Mixed Self-Assembled Monolayer Prepared via a Stepwise Method. Langmuir, 2006, 22, 4885-4889.	3.5	41
94	Aspect ratio control of Au nanorods via temperature and hydroxylamine concentration of reaction medium. Current Applied Physics, 2006, 6, e114-e120.	2.4	14
95	In situ observation of biomolecules patterned on a PEG-modified Si surface by scanning probe lithography. Biomaterials, 2006, 27, 4655-4660.	11.4	42
96	Synthesis oftrans-substituted porphyrin building blocks containing two S-trityl or thiol groups. Korean Journal of Chemical Engineering, 2006, 23, 512-515.	2.7	6
97	Fast heating stage for open liquid-cell atomic force microscopy. Review of Scientific Instruments, 2006, 77, 036114.	1.3	4
98	Multifunctionalization of organosilanes on submicron-sized island-type electrodes for the selective detection of metal ions. Applied Physics Letters, 2006, 88, 013113.	3.3	8
99	Dependence of image distortion in a liquid-cell atomic force microscope on fluidic properties. Applied Physics Letters, 2006, 88, 173121.	3.3	9
100	Fabrication of submicron- or nano-sized mesa electrodes via AFM oxidation: Applications to metal ion detection. Microelectronic Engineering, 2005, 81, 341-348.	2.4	13
101	An array of Au nanoparticles on the nanopatterned Si(100). Microelectronic Engineering, 2005, 81, 389-393.	2.4	8
102	Fabrication of submicron-sized copper structures on pre-patterned self-assembled monolayer and Langmuir-Blodgett films. Korean Journal of Chemical Engineering, 2005, 22, 635-638.	2.7	5
103	Fabrication of submicron size electrode via nonetching method for metal ion detection. Applied Physics Letters, 2005, 86, 073113.	3.3	14
104	In situ Negative Patterning ofp-Silicon via Scanning Probe Lithography in HF/EtOH Liquid Bridges. Journal of the American Chemical Society, 2005, 127, 9380-9381.	13.7	21
105	Response to Comment on "Arsenic Removal Using Mesoporous Alumina Prepared via a Templating Method― Environmental Science & Technology, 2004, 38, 3216-3216.	10.0	0
106	Arsenic Removal Using Mesoporous Alumina Prepared via a Templating Method. Environmental Science & Technology, 2004, 38, 924-931.	10.0	579